

Thermal and Photochemical Nitration of Aromatic Hydrocarbons with Nitrogen Dioxide

E. Bosch and J. K. Kochi*

Chemistry Department, University of Houston, Houston, Texas 77204-5641

Received January 28, 1994*

Aromatic hydrocarbons (ArH) are readily nitrated by nitrogen dioxide (NO₂) in dichloromethane at room temperature and below (in the dark). The red colors, transiently observed, arise from the metastable precursor complex [ArH, NO⁺]NO₃⁻, which is formed in the prior disproportionation of nitrogen dioxide induced by the aromatic donor (eq 7). The deliberate irradiation of the diagnostic (red) charge-transfer absorption band ($h\nu_{CT}$) of [ArH, NO⁺]NO₃⁻ at low temperatures results directly in aromatic nitration, even at -78 °C, where the thermal nitration is too slow to compete. The mechanism of the photochemical (charge-transfer) nitration is established by time-resolved laser spectroscopy to proceed via the aromatic cation radical (ArH^{•+}) formed spontaneously upon the charge-transfer excitation of [ArH, NO⁺]NO₃⁻ in Scheme 1. The related thermal activation of [ArH, NO⁺]NO₃⁻ derives from the adiabatic electron transfer that produces the same radical pair [ArH^{•+}, NO[•]] as the reactive intermediate in Scheme 3. The close relationship between the thermal/photochemical nitrations with nitrogen dioxide and those conventionally carried out with nitric acid (in the presence of nitrous acid) is delineated by Scheme 4.

Introduction

Among the different types of reagents available for the nitration of aromatic hydrocarbons,^{1,2} nitrogen dioxide (NO₂) is particularly versatile owing to its intrinsic paramagnetism and equilibrated dimerization to dinitrogen tetraoxide (N₂O₄).³ Thus, a *free-radical* mechanism for aromatic nitration has been put forward, particularly when nitrogen dioxide is produced in the gas phase⁴ or in nonpolar solvents such as carbon tetrachloride.⁵ On the other hand, the powerful *electrophilic* species, nitrosonium (NO⁺) and nitronium (NO₂⁺), can be generated as reactive intermediates in the ionic dissociation of dinitrogen tetraoxide,⁶ especially in acidic (e.g., H₂SO₄, CF₃CO₂H, etc.) media.⁷ Aromatic nitration with dinitrogen tetraoxide is notably induced by Lewis acids.⁸

Nitration with nitrogen dioxide (dinitrogen tetraoxide) of various aromatic compounds including anisole, methylbenzenes,⁹ and polycyclic aromatics¹⁰ can also be readily

effected in aprotic (nonacidic) media such as dichloromethane, nitromethane, and chloroform. Especially noteworthy is the observation of transient colors of the type originally described for solutions of aromatic hydrocarbons in liquid (neat) dinitrogen tetraoxide.¹¹ Addison and Sheldon¹² correctly ascribed the colors to the presence of 1:1 molecular (addition) complexes but were unable to deduce the relevant structural parameters. Although these workers rejected an ionic structure for aromatic complexes with N₂O₄, our detailed spectroscopic (electronic, vibrational, and time-resolved) studies¹³ were sufficient to assign the transient colors to discrete electron donor-acceptor (EDA) complexes of aromatic hydrocarbons with the nitrosonium cation. These exhibit diagnostic charge-transfer absorptions ($h\nu_{CT}$) in the UV-vis spectrum and characteristic N-O stretching bands in the IR spectrum that relate directly to the ArH/NO⁺ interactions extant in the EDA complexes previously derived from an authentic nitrosonium salt.¹⁴ Such a structural elucidation of the principal intermediate now allows us to describe how the charge-transfer (CT) interactions can provide critical mechanistic insight into aromatic nitrations with NO₂ (N₂O₄).

Results

For the study of aromatic nitrations with nitrogen dioxide, we chose a series of polymethylbenzenes ranging from hexamethylbenzene down to toluene to provide a reactivity range sufficient to delineate the products and stoichiometry for the *thermal* reaction in dichloromethane at 0-25 °C (in the dark). The spectral (UV-vis, IR) examination of the transient colors then revealed the charge-transfer description of the electron donor-acceptor

- * Abstract published in *Advance ACS Abstracts*, May 1, 1994.
 (1) Schofield, K. *Aromatic Nitration*; Cambridge University: Cambridge, 1980.
 (2) Olah, G. A.; Malhorta, R.; Narang, S. C. *Nitration: Methods and Mechanisms*; VCH: New York, 1989.
 (3) (a) Redmond, T. F.; Wayland, B. B. *J. Phys. Chem.* 1968, 72, 1626. (b) James, D. W.; Marshall, R. C. *J. Phys. Chem.* 1968, 72, 2963. (c) Vosper, A. J. *J. Chem. Soc. A* 1970, 2191.
 (4) Titov, A. I. *Tetrahedron* 1963, 19, 557. See also: Olah, G. A. et al. in ref 2, p 88f.
 (5) Squadrito, G. L.; Church, D. F.; Pryor, W. A. *J. Am. Chem. Soc.* 1987, 109, 6535. Squadrito, G. L.; Fronczek, F. R.; Church, D. F.; Pryor, W. A. *J. Org. Chem.* 1989, 54, 548.
 (6) (a) Boughriet, A.; Wartel, M. *J. Chem. Soc., Chem. Commun.* 1989, 809. (b) Bonner, T. G.; Hancock, R. A.; Yousif, G.; Rolle, F. R. *J. Chem. Soc. B* 1969, 1237. See also (c) Cotton, F. A.; Wilkinson, G. *Advanced Inorganic Chemistry*, 5th ed.; Wiley: New York, 1988; pp 324-5.
 (7) (a) Pinck, L. A. *J. Am. Chem. Soc.* 1927, 49, 2536. (b) Goulden, J. D. S.; Millen, D. J. *J. Chem. Soc.* 1950, 2620. (c) Boughriet, A.; Fischer, J.-C.; Wartel, M.; Bremard, C. *Nouv. J. Chim.* 1985, 9, 651. (d) Milligan, B. *J. Org. Chem.* 1983, 48, 1495. Compare also: Olah, G. A.; Malhorta, R.; Narang, S. C. *J. Org. Chem.* 1978, 43, 4628.
 (8) (a) Schaarschmidt, A. Z. *Angew. Chem.* 1926, 1457. Schaarschmidt, A. *Ber.* 1924, 57, 2065. Schaarschmidt, A.; Balzerkiewicz, H.; Gante, H. *Ber.* 1925, 58, 499. (b) Titov, A. I. *J. Gen. Chem. USSR* 1937, 7, 591, 667. (c) Bachman, G. B.; Vogt, C. M. *J. Am. Chem. Soc.* 1958, 80, 2987. (d) Evans, J. C.; Rinn, H. W.; Kuhn, S. J.; Olah, G. A. *Inorg. Chem.* 1964, 3, 857. See also: Bonner, T. G. et al. in ref 6b.
 (9) Underwood, G. R.; Silverman, R. S.; Vanderwalde, A. *J. Chem. Soc., Perkin Trans. 2* 1973, 1177.

- (10) (a) Radner, F. *Acta Chem. Scand.* 1983, B37, 65. (b) Ebersson, L.; Radner, F. *Acta Chem. Scand.* 1985, B39, 343. (c) Ross, D. S.; Hum, G. P.; Schmitt, R. J. In *Polynuclear Aromatic Compounds*; Ebert, L. B., Ed.; American Chemical Society: Washington, D. C., 1988. (d) Pryor, W. A.; Gleicher, G. J.; Cosgrove, J. P.; Church, D. F. *J. Org. Chem.* 1984, 49, 5189. (e) Ebersson, L.; Radner, F. *Acta Chem. Scand.* 1986, B40, 71.
 (11) Addison, C. C. *Chem. Rev.* 1980, 80, 21.
 (12) Addison, C. C.; Sheldon, J. C. *J. Chem. Soc.* 1956, 1941.
 (13) Bosch, E.; Kochi, J. K. *Res. Chem. Intermed.* 1993, 19, 811.
 (14) Kim, E. K.; Kochi, J. K. *J. Am. Chem. Soc.* 1991, 113, 4962.

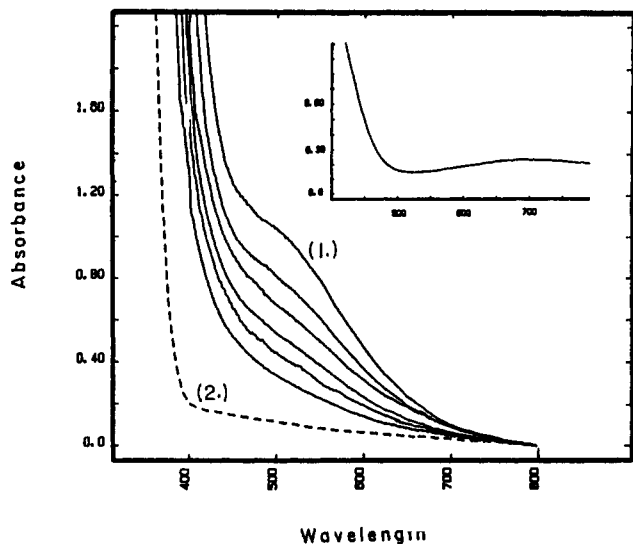
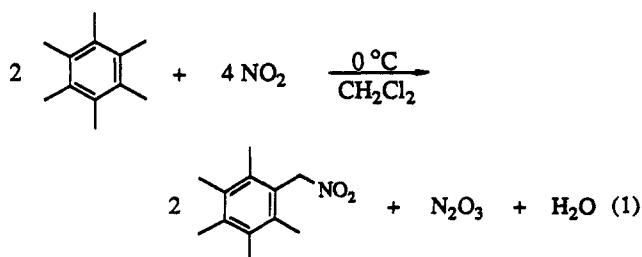


Figure 1. Temporal change in the charge-transfer absorption of 0.075 M hexamethylbenzene and 0.2 M nitrogen dioxide in dichloromethane at 0 °C; spectrum 1, upon mixing and others measured at 5, 12, 20, 40, and 60 min; spectrum 2, 0.2 M nitrogen dioxide alone. Inset: spectrum of bleached solution (after 2 h) cooled to -78 °C showing the broad absorption of N_2O_3 with $\lambda_{max} = 690$ nm.

(EDA) precursor complexes of aromatic hydrocarbons with nitrogen dioxide. The corresponding *photochemical* nitration was thus carried out by activating the EDA complexes via the irradiation of the charge-transfer absorptions at low temperatures (-78 °C), where the thermal nitration was too slow to compete.¹⁵

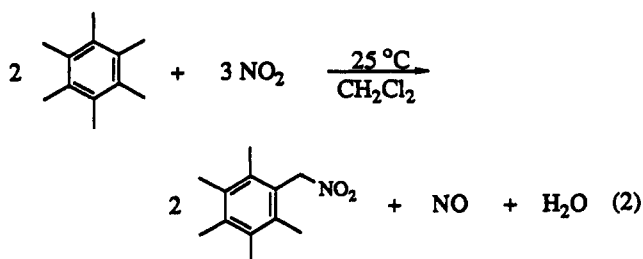
I. Thermal Nitration of Various Methylarenes with Nitrogen Dioxide. Addition of hexamethylbenzene to a pale yellow solution of nitrogen dioxide (~0.1 M) in dichloromethane under an argon atmosphere resulted immediately in an intense red-brown coloration. The subsequent bleaching of the solution in the dark, even at 0 °C, is illustrated in Figure 1 by the monotonous decrease of the low-energy absorbance in the spectral region between 400 and 700 nm. Spectral examination of the residual solution cooled to -78 °C after 2 h (see inset, Figure 1) showed a broad, weak absorption band with $\lambda_{max} = 690$ nm, diagnostic of dinitrogen trioxide.¹⁶ Aqueous workup, followed by HPLC and GC-MS analysis, indicated the side-chain substituted (pentamethylphenyl)nitromethane to be the principal product according to the stoichiometry in eq 1. When the same reaction was carried out at room



(15) Coloration due to EDA complex formation is also observed in other aprotic solvents including chloroform, nitromethane, and acetonitrile. Dichloromethane was considered the solvent of choice since a low-melting solvent was required to perform the comparable photochemical nitration at a temperature (-78 °C) where the thermal nitration was completely suppressed.

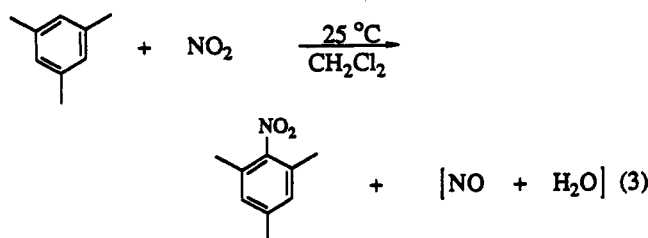
(16) Shaw, A. W.; Vosper, A. J. *J. Chem. Soc., Dalton Trans.* 1972, 961.

temperature, the metastable dinitrogen trioxide reacted further and it was completely converted to nitric oxide, *i.e.*

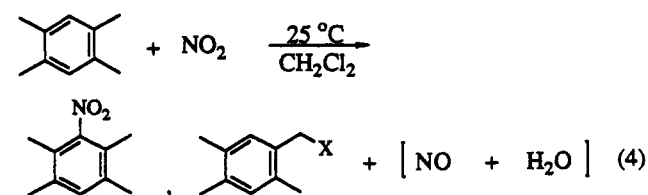


The stoichiometry in eq 2 was qualitatively confirmed by the characteristic (gas-phase) spectrum of only nitric oxide¹⁷ (with no admixture of NO_2) over the solution. [Note that the homolytic dissociation of N_2O_3 to NO and NO_2 is significant above 0 °C, being 80% dissociated at 25 °C.¹⁸]

The color changes accompanying the exposure of mesitylene to nitrogen dioxide in dichloromethane at 25 °C were much like those illustrated in Figure 1. However, the workup and analysis of the decolorized solution after 6 h (in the dark) indicated that ring nitration was the exclusive course of reaction, *i.e.*



The treatment of pentamethylbenzene and durene with nitrogen dioxide under similar conditions led to mixtures of ring and side chain nitro derivatives in the varying proportions listed in Table 1, *e.g.*



where X = NO_2 and ONO_2 . (Control experiments showed that benzylic nitrites were readily converted to the corresponding nitrates under the conditions of the experiment, as described in the Experimental Section.) In addition, small amounts of (1,1',2,3',4,4',5-heptamethyldiphenyl)methane^{19a} (where X = 2,3,5,6-tetramethylbenzyl in eq 4) and the analogous dimeric (nonamethyldiphenyl)methane^{19b} were byproducts in the nitration of durene and pentamethylbenzene, respectively (see Table 1). The dimeric hydrocarbon²⁰ 4,4'-dimethyl-1,1'-dinaphthyl was

(17) (a) Fateley, W. G.; Bent, H. A.; Crawford, B., Jr. *J. Chem. Phys.* 1959, 31, 204. (b) For the stoichiometry of the reaction of pyrene and perylene with nitrogen dioxide in dichloromethane see: Ebersson, L. et al. in ref 10b.

(18) Beattie, I. R.; Bell, S. W. *J. Chem. Soc.* 1957, 1681.

(19) (a) Hanna, S. B.; Hunziker, E.; Saito, T.; Zollinger, H. *Helv. Chim. Acta* 1969, 52, 1537. (b) Hunziker, E.; Myhre, P. C.; Penton, J. R.; Zollinger, H. *Helv. Chim. Acta* 1975, 58, 230.

(20) Compare Radner, F. *J. Org. Chem.* 1988, 53, 702.

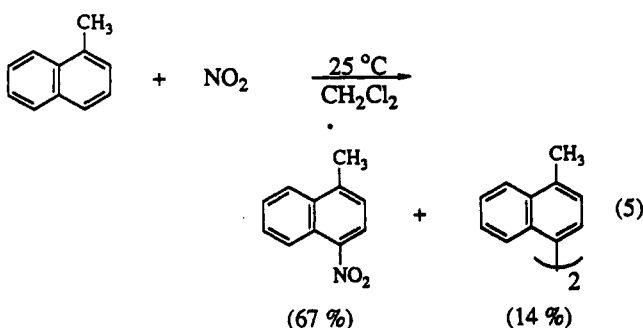
Table 1. Thermal Nitration of Polymethylbenzenes with Nitrogen Dioxide^a

methyl- arene ^b ArCH ₃	products, ^c %			convn, ^d %	temp/time, °C/h
	ArNO ₂	ArCH ₂ NO ₂	ArCH ₂ ONO ₂		
HMB		73	27 ^e	20	0/1.0
PMB	18	18	42 ^f	37	25/0.75
PMB ^g	44	31	19 ^h	8	25/0.75
DUR	2	30	64 ⁱ	75	25/1.5
DUR ^j	4	41	49 ^h	88	25/1.5
MES	100	l	l	74	25/24
MES ^m	100	l	l	12	25/24
MES ⁿ	100	l	l	27	25/24
<i>m</i> -XYL	100 ^p	l	l	17	25/10

^a In dichloromethane at 25 °C, unless indicated otherwise.

^b Hexamethylbenzene = HMB, pentamethylbenzene = PMB, durene = DUR, mesitylene = MES, *m*-xylene = *m*-XYL. ^c Molar distribution of products based on recovered aromatic hydrocarbon where ArH = ArCH₃. ^d Conversion based on recovered methylarene. ^e Includes ArCH₂OH (7%). ^f In addition, (nonamethyldiphenyl)methane (NP) formed (22%). ^g Under NO atmosphere (see Experimental Section). ^h In addition, (heptamethyldiphenyl)methane HM formed (6%). ⁱ In addition, HM (4%) and 2,4,5-trimethylbenzaldehyde TB (1%) formed. ^j In nitroethane solvent. ^k In addition, HM (3%) and TB (1%) formed. ^l Below detection limits. ^m With added tetrabutylammonium nitrate (1 equiv). ⁿ With added 4-methyl-2,6-di-*tert*-butylpyridine (1 equiv). ^p As a 92:8 mixture of 4-nitro- and 2-nitro-*m*-xylene.

also a significant byproduct in the nitration of α -methyl-naphthalene with nitrogen dioxide,^{10e} *i.e.*



Although *m*-xylene afforded the ring-nitrated dimethylnitrobenzenes in high yields (Table 1, last entry), the isomeric *o*- and *p*-xylenes produced complex mixtures derived from both ring and side chain substitution, as well as oxidation products—including the nitroxylenes, α -nitrotoluenes, benzyl alcohols, benzaldehydes, etc. The yellow-orange solution of the toluene and nitrogen dioxide persisted for prolonged periods (in the dark), and toluene could be recovered in essentially quantitative yields.

The reactivity of the various polymethylbenzenes toward nitrogen dioxide qualitatively increased with the number of methyl substituents. Thus, hexamethylbenzene and pentamethylbenzene reacted most readily even with dilute solutions of NO₂ in dichloromethane, as visually indicated by the rapid discharge of the dark red-brown colors at ice bath temperatures. Durene, mesitylene, and xylene afforded progressively less intensely colored solutions, and the rates of decolorization became correspondingly slower. As a result, the reactions were performed at room temperature with higher concentrations of nitrogen dioxide in order to effect reasonable conversions within the limited time spans listed in Table 1. Since all of these colors persisted indefinitely when the solutions were merely cooled to -78 °C and protected from light (especially adventitious roomlight), the chemical transformations in

Table 2. Promotion of Benzene Nitration with Lewis Acids and Nitrosonium^a

benzene, mmol	NO ₂ , mmol (M)	additive, mmol	time, h	C ₆ H ₅ NO ₂ , mmol	C ₆ H ₆ , ^b mmol	M.B., %
22.41	63.0 (10.5)	none	78	0.07	19.10	87
11.20	15.8 (2.88)	SbCl ₅	0.50	38	2.31	6.52
11.20	15.8 (2.88)	SbCl ₅	1.00	38	4.20	5.21
11.20	25.2 (2.86)	AlCl ₃	1.04	66	2.70	6.00
11.20	25.2 (2.86)	FeCl ₃	0.99	66	2.30	6.40
11.20	25.2 (2.86)	NOSbCl ₆	0.93	50	2.54	6.90

^a In dichloromethane at 25 °C. ^b Amount recovered.

Table 1 that accompany the color changes are arbitrarily referred to hereafter as *thermal nitrations*.

Although the gaseous nature of the nitrogen oxides discouraged a rigorous kinetics study, three qualitative observations on reactivity are particularly noteworthy. Thus, aromatic nitrations carried out with NO₂ showed signs of autoretardation by the reduced nitric oxide, as follows. Dark red solution of pentamethylbenzene (PMB) and NO₂ in dichloromethane were prepared in duplicate at -78 °C. Significant diminution of the red color was observed when the argon atmosphere was replaced by NO; and the concomitant development of a green tinge signified the formation of dinitrogen trioxide.¹⁶ When both solutions were allowed to react at 25 °C (in the dark), the PMB conversion of 62% (under argon) was found to be diminished to only 10% in the presence of nitric oxide (compare entries 2 and 3 in Table 1). A similar retardation was noted when 1 equiv of either nitrate (as the tetrabutylammonium salt) or a pyridine base was present during the nitration of mesitylene (see Table 1, entries 7 and 8). In each case, the rate retardation induced by the additive coincided with the initial attenuation of the color intensity—the diminished red colors leading to lower conversions (column 5, Table 1).

The direct relationship between (rate) conversion and (color) intensity also extended to the *promotion* of aromatic nitration with Lewis acids.^{6b,8} For example, the yellow color of a dichloromethane solution of benzene and nitrogen dioxide persisted unchanged over a 24-h period, and the conversion to nitrobenzene was found to be less than 1% at room temperature (Table 2). By contrast, the presence of antimony pentachloride (3 mol % relative to NO₂) led to a dark orange solution that afforded 20% nitrobenzene (entry 2), under otherwise identical conditions. The presence of more SbCl₅ (6 mol %) led to a deeper orange solution and a correspondingly higher conversion (40%) to nitrobenzene (Table 2, entry 3). The promotion by Lewis acids was even more pronounced with toluene, as indicated by the dramatic deepening of the color from yellow to red with successive increments of SbCl₅ that paralleled the increasing conversion from less than 1% to more than 60% nitrotoluene, as described in Table 3. The product distribution among the isomeric nitrotoluenes remained relatively invariant throughout the range of added SbCl₅. The linear increase in conversion to the nitrotoluenes with the added Lewis acid is illustrated in Figure 2. It is especially noteworthy that the same increase in conversion was induced by the addition a nitrosonium salt (NO⁺SbCl₆⁻) to nitrogen dioxide (see Table 2, entry 6, and Table 3, entries 11 and 12).

II. Spectral Characterization of the Transient EDA Complexes of Aromatic Hydrocarbons with Nitrogen Dioxide. The distinctive colorations observed immediately upon the mixing of nitrogen dioxide (dini-

Table 3. Effect of Lewis Acids and Nitrosonium on the Nitration of Toluene with Nitrogen Dioxide^a

NO ₂ , mmol (M)	solvent ^b	additive, mmol		products, mmol			rec., ^c mmol	yield, %
				<i>o</i> -	<i>p</i> -	<i>m</i> -		
19.0 (2.6)	MC	SbCl ₅	0.20	0.13	0.15	0.002 ^d	6.80	3.2
20.0 (2.8)	MC	SbCl ₅	0.50	0.64	0.74	<0.03	7.20	15
19.0 (2.4)	MC	SbCl ₅	1.00	1.26	1.47	0.03	6.10	29
19.0 (2.4)	MC	SbCl ₅	2.00	2.80	2.74	0.05	4.16	59
19.0 (2.6)	NM	SbCl ₅	0.50	1.35	0.85	<0.05	7.28	23
15.6 (2.4)	AN	SbCl ₅	0.25	0.48	0.24	0.02	5.39	12
18.8 (2.0)	MC	AlCl ₃	0.93	0.73	0.71	0.02	7.00	16
18.8 (2.8)	AN	AlCl ₃	0.94	0.56	0.23	0.03	7.80	9
18.8 (2.0)	MC	FeCl ₃	0.96	0.36	0.29	0.01	7.08	7
18.8 (2.0)	MC	PCl ₅	1.10	0.03	0.02		7.10	0.5
19.0 (2.4)	MC	NOSbCl ₆	0.94 ^e	0.70	0.62	0.06	7.35	15
18.8 (2.8)	MC	NOBF ₄	1.00 ^f		<0.02		8.50	

^a With 9.4 mmol of toluene at 25 °C for 24 h. ^b Dichloromethane = MC, nitromethane = NM, acetonitrile = AN. ^c Recovered toluene. ^d Phenylnitromethane (0.015 mmol) also formed. ^e Partially soluble. ^f Insoluble.

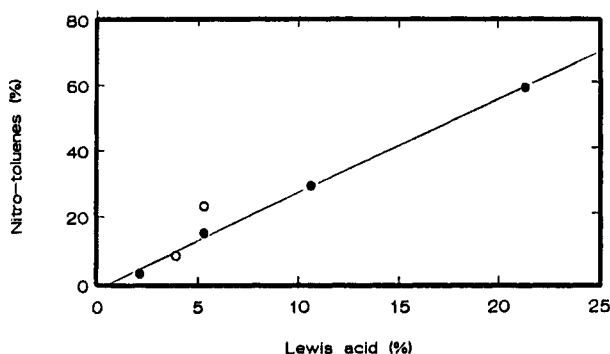
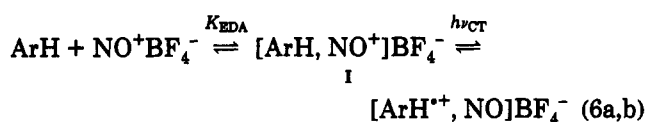


Figure 2. Effect of antimony pentachloride on the molar conversion (after 24 h) of 1.4 M toluene and 2.8 M nitrogen dioxide to (combined) nitrotoluenes at 25 °C in either dichloromethane (●) or nitromethane (○).

trogen tetroxide) with the benzenoid substrates in Table 1 were strongly dependent on the number of methyl substituents. Thus, intense red-brown colors could be produced from 0.1 M hexamethylbenzene, while comparable colorations were obtained with the slower reacting mesitylene only at significantly higher (1 M) concentrations. Moreover, at the latter levels, the corresponding xylene solutions were merely pink. Spectral (UV-vis) examination of the colored solutions showed distinctive new absorption bands of the type previously assigned to the charge-transfer excitation ($h\nu_{CT}$) of the intermolecular (1:1) electron donor-acceptor or EDA complexes I of the nitrosonium salt NO^+BF_4^- with the corresponding aromatic donors,¹⁴ *i.e.*



The spectral similarity is apparent in Table 4 by the pairwise comparisons of the charge-transfer absorptions of NO^+BF_4^- and NO_2 (N_2O_4) with some representative methylarenes. The spectral coincidence of the two systems is not fortuitous, since it is further underscored in Table 4 by the quantitative comparisons of the diagnostic N–O stretching frequencies (ν_{NO}) in both series of infrared spectra (last column). The bathochromic shifts (together with the strongly varying intensities) of the charge-transfer and N–O stretching bands relate to the strong dependence previously established¹⁴ for the complexation constant

Table 4. Spectral (UV-vis, IR) Comparison of the Charge-Transfer Absorptions of Aromatic Complexes with NO_2 (N_2O_4), NO^+BF_4^- , and NO_2 (SbCl_6^-)

aromatic donor	I.P., ^a eV	acceptor	$h\nu_{CT}$ (fwhm), ^b nm, 10^2 cm^{-1}	ν_{NO} (fwhm), ^c cm^{-1}
hexamethylbenzene	7.85	NO_2 (N_2O_4)	495 (59)	1862 (48)
		NO^+BF_4^-	499 (57)	1885 (52)
		NO_2 (SbCl_6^-)	499 (60)	1850 (49)
hexaethylbenzene	7.71	NO_2 (N_2O_4)	516 (57)	1900 (53)
		NO^+BF_4^-	511 (103)	1896 (55)
pentamethylbenzene	7.92	NO_2 (N_2O_4)	491 (69)	1907 (65)
		NO_2 (SbCl_6^-)	490 (75)	
durene	8.05	NO_2 (N_2O_4)	486 (67)	1948 (53)
		NO^+BF_4^-	486 (67)	1975 (74)
		NO_2 (SbCl_6^-)	489 (59)	1880 (63)
mesitylene	8.42	NO_2 (N_2O_4)	486 (67)	1948 (53)
		NO^+BF_4^-	486 (67)	1975 (74)
		NO_2 (SbCl_6^-)	493 (52)	1954 (30)
<i>p</i> -xylene	8.44	NO_2 (N_2O_4)	496 (116)	1964 (57)
		NO^+BF_4^-	496 (116)	1998 (92)
		NO_2 (SbCl_6^-)	506 (61)	

^a From ref 21. ^b Maximum of low-energy band [$h\nu_{CT}(\text{II})$ in ref 14] in dichloromethane solution at -78 °C (in parentheses, fwhm = full width at half maximum). ^c IR spectra of aromatic EDA complex with NO_2 (N_2O_4) in dichloromethane solution at -78 °C, NO^+BF_4^- in nitromethane solution at 25 °C (from ref 14), and NO_2 (SbCl_6^-) in Nujol mull at 25 °C.

K_{EDA} of NO^+ in eq 6a on the aromatic donor strength, as evaluated by the ionization potential (see Table 4, column 2).²¹ Accordingly, the CT colorations were readily assigned to the relevant ArH/ NO^+ interactions in the aromatic EDA complex II resulting from the (induced) disproportionation of nitrogen dioxide (dinitrogen tetroxide), *i.e.*¹³



The ionic disproportionation of nitrogen dioxide (dinitrogen tetroxide) in the EDA complex II derives its principal driving force from the charge-transfer (π) complexation of the nitrosonium (NO^+) moiety according to eq 7 (brackets).¹⁴ The magnitude of this driving force $-\Delta G^\circ_{\text{DISP}}$ was evaluated from the series of temperature-dependent spectral changes (Figure 3) attendant upon the progressive lowering of the temperature of a dichloromethane solution of mesitylene and nitrogen dioxide from 25 °C (pale orange) to -78 °C (deep red). In this

(21) Howell, J. O.; Goncalves, J. M.; Amatore, C.; Klasinc, L.; Wightman, R. M.; Kochi, J. K. *J. Am. Chem. Soc.* 1984, 106, 3968.

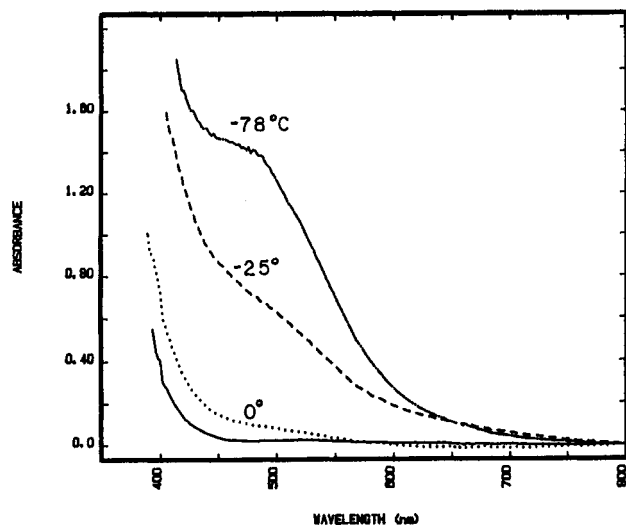


Figure 3. Temperature-dependent CT spectrum of 1.5 M mesitylene and 0.2 M nitrogen dioxide in dichloromethane at 25, 0, -25, and -78 °C.

Table 5. Free Energy of Formation of the Charge-Transfer Complex from Mesitylene and Nitrogen Dioxide^a

temperature (°C)	0	-25	-50	-78
K_{DISP}^b (10^2 M^{-1})	1.0	6.8	7.5	15
$\Delta G^{\circ}_{\text{DISP}}$ (kcal mol ⁻¹)	2.5	1.3	1.1	0.7

^a Based on $\epsilon_{\text{CT}} = 210 \text{ M}^{-1} \text{ cm}^{-1}$ at $\lambda_{\text{max}} = 475 \text{ nm}$ ¹⁴ for the EDA complex from 0.5 M mesitylene and 0.2 M nitrogen dioxide in dichloromethane. ^b For eq 7.

treatment, the values of K_{DISP} in Table 5 were calculated at each temperature from the extinction coefficient of $\epsilon_{\text{EDA}} = 210 \text{ M}^{-1} \text{ cm}^{-1}$ that was previously measured for the EDA complex with ArH = mesitylene in eq 6b.²² The facile reversibility of the disproportionation in eq 7 was also evident in the rapid discharge of the charge-transfer absorption of II merely upon the addition of nitric oxide—the equilibrium shift to the left resulting from the depletion of NO_2 by its rapid homolytic combination with NO to form dinitrogen trioxide¹⁶ (see Experimental Section).

Ionic disproportionation of NO_2 (N_2O_4) can also be promoted in nonpolar media by the addition of Bronsted and Lewis acids.²³ Such an acid-induced process was conveniently observed by a marked (hypochromic) increase in the color intensity—most dramatically in solutions containing only weak (or relatively electron-poor) aromatic donors. For example, a dilute solution of durene (DUR, 10 mM) showed little visible evidence of charge-transfer colors when exposed to 2 mM nitrogen dioxide at -78 °C in dichloromethane.²⁴ [Note for comparison the intense red solutions easily obtained with hexamethylbenzene under comparable conditions.] However, the addition of small quantities of antimony pentachloride (typically 1.0 mM) to the (essentially) colorless solution resulted spontaneously in the intense absorption spectra of the [DUR, NO^+] complex,¹⁴ as illustrated in Figure 4. The inset to Figure 4 confirms the Lewis-acid promotion of the charge-transfer interaction between durene and NO^+

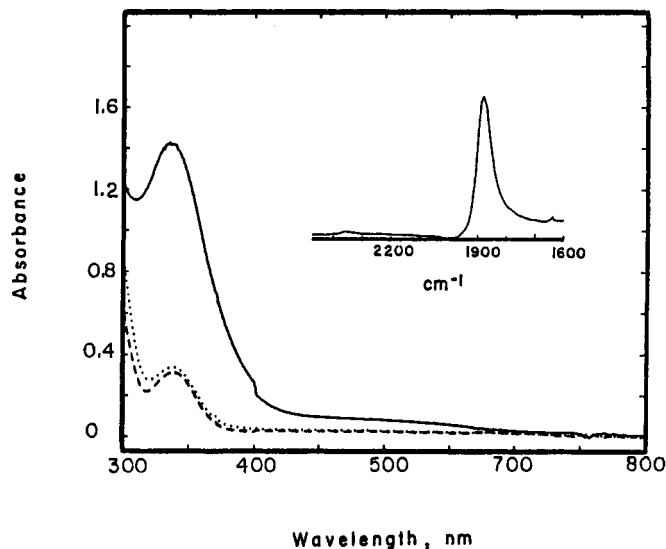
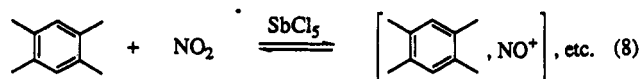


Figure 4. Lewis-acid enhanced CT spectrum (—) of the nitrosonium EDA complex from the addition of 0.001 M SbCl_5 to a solution of 0.01 M durene and 0.002 M nitrogen dioxide (\cdots) in dichloromethane at -78 °C. Nitrogen dioxide alone (---). Inset: IR spectrum of the durene EDA complex with nitrogen dioxide showing $\nu_{\text{NO}} = 1880 \text{ cm}^{-1}$.

by the presence of the diagnostic N–O stretching band¹⁴ at $\nu_{\text{NO}} = 1880 \text{ cm}^{-1}$, *i.e.*



The direct correspondence between the aromatic CT energies ($h\nu_{\text{CT}}$) obtained with NO_2 under these (Lewis) acidic conditions and those obtained with NO^+BF_4^- is also given in Table 4 (column 4) for mesitylene and *p*-xylene, as well as hexamethylbenzene and pentamethylbenzene.

In order to identify the relevant role of Lewis acids on the reduction of NO_2 in eq 8, 1 equiv of SbCl_5 was added at -78 °C to a deep red solution containing equimolar amounts of hexamethylbenzene (HMB) and nitrogen dioxide in dichloromethane. After the addition of *n*-hexane, the dense brick-red precipitate III was separated by filtration, washed with cold dichloromethane, and dried in vacuo. Analysis of the mother liquors indicated that essentially all the hexamethylbenzene was accounted for as III. Similar results were obtained with durene, mesitylene and *p*-xylene. In all cases, repeated attempts to grow single crystals of the metastable red solids that were suitable for X-ray crystallography invariably led to (partial) decomposition. However, the solid-state IR analysis of III (Nujol) was sufficient to reveal the pertinent CT interaction of nitrosonium²⁵ by the diagnostic N–O stretching band at $\nu_{\text{NO}} = 1850 \text{ cm}^{-1}$ for [HMB, NO^+] in Table 4, and from the three characteristic IR bands of the unidentate (C_{2v}) nitrate²⁶ at 1445 cm^{-1} (antisymmetric NO_2 stretch), 1297 cm^{-1} (symmetric NO_2 stretch), and 1063

(22) By taking the value of ϵ_{EDA} to be invariant with temperature.¹⁴

(23) Goulden, J. D. S.; Millen, D. J. *J. Chem. Soc.* 1950, 2620. See also: Addison, C. C. in ref. 11. Bonner, T. G. et al. in ref. 6b.

(24) Owing to the facile monomer/dimer equilibrium, concentrations are arbitrarily given in terms of either nitrogen dioxide or dinitrogen tetraoxide, *i.e.*, 2 equiv of $\text{NO}_2 = 1$ equiv of N_2O_4 .

(25) The relevant CT interaction in the brick red solid is also indicated in the ¹³C NMR spectrum by the strongly shifted resonances at δ 147.7 (aromatic) and 17.8 (methyl) relative to those of free HMB (δ 132.5, 16.8).¹⁴

(26) Addison, C. C.; Logan, N.; Wallwork, S. C.; Garner, S. C. *Quart. Rev.* 1971, 25, 289.

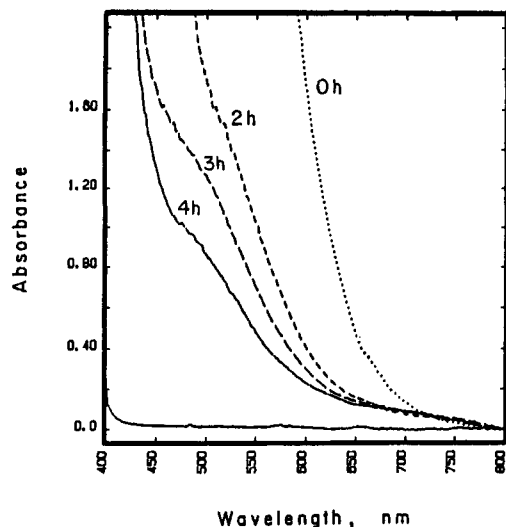
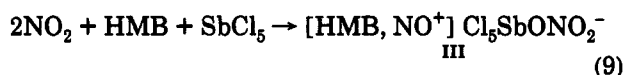


Figure 5. Photobleaching of the charge-transfer absorption from 0.18 M mesitylene and 0.5 M nitrogen dioxide in dichloromethane by irradiation with $\lambda_{\text{exc}} > 415$ nm at -78 °C.

cm^{-1} (NO stretch),²⁷ we inferred the Lewis-acid coordination to nitrate in the EDA complex III as



Thus, the transient EDA complexes II and III derived from methylarenes and nitrogen dioxide in the absence and presence of a Lewis acid, respectively, share in common the relevant ArH/NO^+ interaction that is central to the parent complex I prepared from the authentic nitrosonium salt in eq 6a.¹⁴

III. Photochemical Nitration of Methylarenes with Nitrogen Dioxide via the Selective Activation of the EDA Complex. Since the ArH/NO^+ interaction was common to every aromatic EDA complex with NO_2 in Table 4, the complexes were selectively activated by the deliberate irradiation of the charge-transfer absorption bands. Owing to the thermal stability of all the aromatic EDA complexes at -78 °C, the colored solutions were directly irradiated at this low temperature with filtered (visible) light chosen to excite only the low-energy tails of the charge-transfer bands (compare Figure 1). Experimentally, the selective excitation was achieved with actinic radiation from a 500-W mercury lamp equipped with a sharp cutoff filter so that only light with $\lambda_{\text{exc}} > 415$ nm was transmitted. Thus, under these controlled conditions, there could be no ambiguity about the adventitious excitation of either the uncomplexed methylarene or nitrogen dioxide (compare Figure 1). Accordingly, the photochemical transformations carried out in this manner are hereafter designated as *charge-transfer nitrations* in the following way.

The photoactivation of the EDA complex of mesitylene (0.06 M) with nitrogen dioxide (0.05 M) at -78 °C resulted in the steady bleaching of the CT color over the course of several hours, as illustrated in Figure 5. An identical solution was also prepared but kept protected from light at the same temperature alongside the irradiated solution. The simultaneous workup of this (dark) control and the

Table 6. Charge-Transfer Nitration of Polymethylbenzenes with Nitrogen Dioxide^a

methylarene ^b ArCH ₃	products, ^c %			convn, ^d %	time, ^d h
	ArNO ₂	ArCH ₂ NO ₂	ArCH ₂ ONO ₂		
HMB		49	51	80	6.5
PMB	7	31	61 ^e	90	11.5
DUR	1	18	73	74	17
DUR ^f	20	12	54 ^h	54	48
MES	100	0		18	3
TMB	100	0		14	22
<i>m</i> -XYL	100 ⁱ	0		41	4
<i>o</i> -XYL	100 ^j			2	6

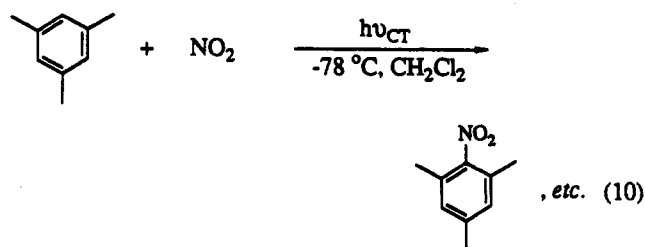
^a In dichloromethane solution at -78 °C by irradiation with $\lambda_{\text{exc}} > 415$ nm, unless indicated otherwise. ^b See footnote b, Table 1. TMB = 1,2,4-trimethylbenzene, *o*-xylene = *o*-XYL. ^c See footnote c, Table 1. ^d Conversion based on recovered methylarene. ^e Includes 2,3,4,5-tetramethylbenzyl nitrite. In addition, traces of (nonamethyldiphenyl)methane (NDM) detected (<1%). ^f In addition, (heptamethyldiphenyl)methane, HDM (4%), and 2,4,5-trimethylbenzaldehyde, TB (4%), formed. ^g In nitroethane solvent at -78 °C. ^h In addition, TB (1%), HDM (8%), and various nitro- and nitrate-DPM's (4%) formed. ⁱ As a 97:3 mixture of 4-nitro- and 2-nitro-*m*-xylene. ^j As a 89:11 mixture of 4-nitro- and 3-nitro-*o*-xylene.

Table 7. Quantum Yield for Charge-Transfer Nitration with Nitrogen Dioxide^a

methylarene (M)	NO ₂ , M	quantum yield, %
hexamethylbenzene (0.06)	0.4	0.02
pentamethylbenzene (0.07)	0.4	0.10
mesitylene (0.18)	2.0	0.11

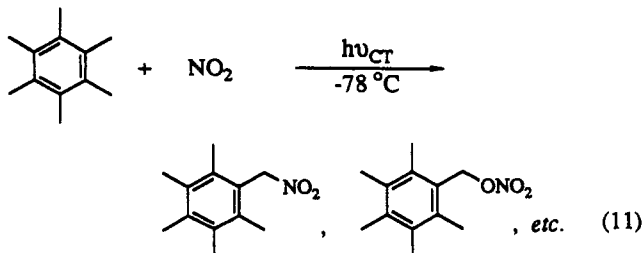
^a In dichloromethane solution at -70 °C (see Experimental Section).

photolysate (see Experimental Section) was followed by quantitative GC-MS and HPLC analysis using the internal standard method. Although mesitylene was quantitatively recovered from the unirradiated solution, analysis of the bleached photolysate in Table 6 showed that it was converted to nitromesitylene in 84% yield, *i.e.*



The photoefficiency of the charge-transfer nitration in eq 10 was determined by ferrioxalate actinometry with monochromatic light at $\lambda_{\text{exc}} = 440$ nm (see Experimental Section), and the quantum yield for the production of nitromesitylene was found to be $\Phi_{\text{P}} = 0.11$ (Table 7).

The photochemical transformation of the hexamethylbenzene EDA complex under the same conditions led to side chain substitution in the manner described (Table 1) for the thermal process, *i.e.*



It is noteworthy that the quantum efficiency for side chain

(27) (a) Laane, J.; Ohlsen, J. R. *Prog. Inorg. Chem.* 1980, 27, 466. (b) Nakamoto, K. *Infrared and Raman Spectra of Inorganic and Coordination Compounds*, 4th ed.; Wiley: New York, 1986.

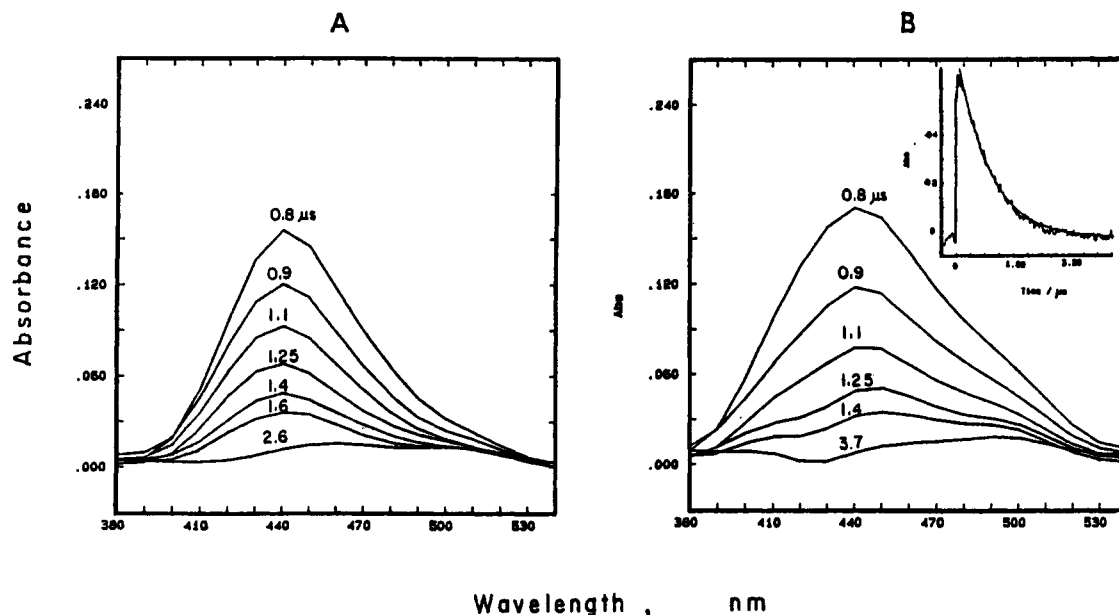
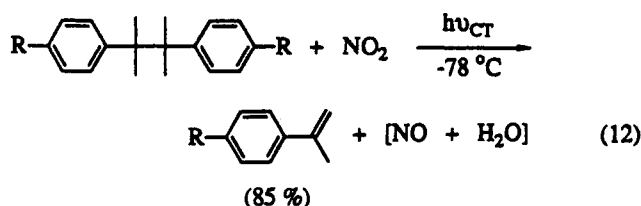


Figure 6. Temporal evolution of the spectral transients from the hexamethylbenzene and (A) $\text{NO}^+ \text{BF}_4^-$ or (B) NO_2 (N_2O_4) in dichloromethane (at -78°C) measured at the indicated times following the 532-nm excitation with a 10-ns laser pulse. Inset: spectral decay at 432 nm with the smooth curve representing the first-order fit with $k_{\text{bet}} = 1.1 \times 10^6 \text{ s}^{-1}$.

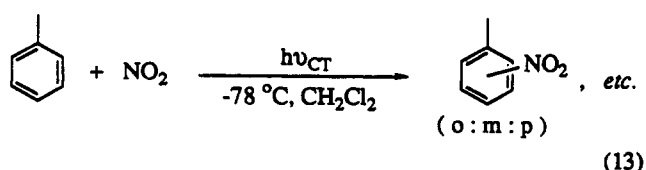
substitution according to eq 11 was substantially less than that for nuclear nitration (Table 7).

The CT photoactivation of durene and pentamethylbenzene could be carried out in high conversion to product mixtures derived from both side chain and ring nitration (see Table 6, entries 3, 4, and 2, respectively) that were strongly reminiscent of those obtained in thermal nitration (eq 4). Similarly, the charge-transfer nitration of 1,2,4-trimethylbenzene and *m*-xylene yielded mainly ring-nitrated products (entries 6 and 7), whereas *p*-xylene afforded a complex mixture of 2-nitro- and α -nitro-*p*-xylene as well as 4-methylbenzyl alcohol and aldehyde (see Experimental Section). Solutions of either bicumene or 4,4'-dimethylbicumene and nitrogen dioxide in dichloromethane at -78°C exhibited pale red absorptions similar to the charge-transfer bands of the xylene complexes with NO_2 . Selective irradiation at $\lambda_{\text{exc}} > 415 \text{ nm}$ for 2 h at -78°C yielded a single (styrene) product corresponding to the oxidative cleavage of the aromatic donor, *i.e.*



where $\text{R} = \text{H}, \text{CH}_3$. The absence of the ring-substituted nitrocumenes (<1%) was particularly striking.

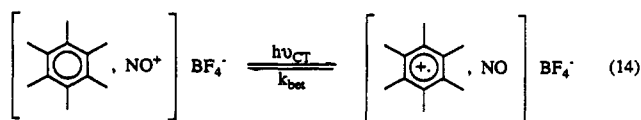
The orange solution obtained at high concentrations of toluene and nitrogen dioxide in dichloromethane was slowly converted at -78°C to a mixture of *o*-, *m*-, and *p*-nitrotoluene, *i.e.*



together with minor products derived from side chain substitution (α -nitrotoluene) and oxidation (benzaldehyde). Under similar photochemical conditions, benzene and nitrogen dioxide were inefficiently converted to nitrobenzene, together with an isomeric mixture of dinitrobenzenes (see Experimental Section).

IV. Time-Resolved Spectra from the Charge-Transfer Excitation of Aromatic EDA Complexes with Nitrogen Oxides. Charge-transfer in the ground state of the nitrosonium complex I (as formed in eq 6a) has its excited-state counterpart that is deliberately induced by vertical excitation of the EDA complex in eq 6b.²⁸ Thus, the laser pulse at $\lambda_{\text{exc}} = 532 \text{ nm}$ corresponding to the second harmonic of a Q-switched Nd^{3+} :YAG laser was well suited for the specific excitation of the charge-transfer bands derived from various aromatic donors and nitrogen oxides, as judged from the magnitudes of $h\nu_{\text{CT}}$ in Table 4.

The time-resolved absorption spectrum in Figure 6A was obtained at -78°C upon the application of a 10-ns (fwhm) laser pulse at $\lambda_{\text{exc}} = 532 \text{ nm}$ to a dichloromethane solution of the authentic hexamethylbenzene EDA complex prepared from the nitrosonium salt $\text{NO}^+ \text{BF}_4^-$ in eq 6a. The location and distinctive shape of the 10-ns transient corresponded to that of the hexamethylbenzene/nitric oxide radical ion pair.²⁹ The subsequent decay of the transient absorption (for return to the spectral base line) followed first-order kinetics. The rate constant of $k_{\text{bet}} = 1.1 \times 10^6 \text{ s}^{-1}$ corresponded to the temporal relaxation of the radical ion pair by back-electron transfer to regenerate the EDA complex, *i.e.*¹³



(28) Kochi, J. K. *Adv. Phys. Org. Chem.* 1993, 29, 185.

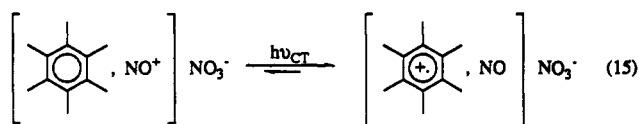
(29) Bockman, T. M.; Karpinski, Z. J.; Sankararaman, S.; Kochi, J. K. *J. Am. Chem. Soc.* 1992, 114, 1970.

Table 8. Formation of Arene Cation Radicals on the Selective Charge-Transfer Excitation of Various Methylbenzene EDA Complexes with NO₂ and NO⁺BF₄⁻ ^a

methylarene donor	acceptor	
	NO ₂ λ _{max} , ^b nm	NO ⁺ BF ₄ ⁻ λ _{max} , ^b nm
hexamethylbenzene	440 ± 10	430 ± 5
pentamethylbenzene	450 ± 5	450 ± 5
durene	440 ^c ± 10	430 ± 10
p-xylene	440 ^c ± 10	

^a In dichloromethane solution cooled to -78 °C. Excitation wavelength, λ = 532 nm. ^b Absorption maximum of the arene cation radical. ^c Approximate value.

The same laser pulse with λ_{exc} = 532 nm was also used to excite the hexamethylbenzene EDA complex formed with nitrogen dioxide (eq 7), under otherwise identical conditions. Most importantly, the time-resolved spectrum shown in Figure 6B was indistinguishable from that generated via the nitrosonium acceptor, *i.e.*

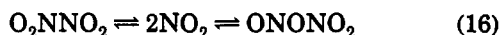


Moreover, the decay pattern indicated that the microsecond lifetime of the radical ion pair in eq 15 was comparable to that derived from NO⁺BF₄⁻ in eq 14.

Transient spectra of radical cations from other aromatic complexes prepared from either the nitrosonium (NO⁺) or the nitrogen dioxide (NO₂) acceptor are directly compared in Table 8. Clearly, the excited-state properties of the charge-transfer complexes derived from nitrogen dioxide were the same as those from the authentic nitrosonium complex. This provides further substantiation that the coloration observed upon the treatment of aromatic donors with nitrogen dioxide is accurately described by the (quasi) photostationary state (shown in brackets) in eq 15.

Discussion

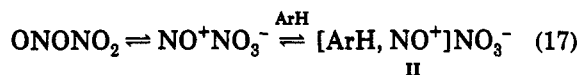
I. Formation of Nitrosonium EDA Complexes from Aromatic Hydrocarbons and Nitrogen Dioxide. The combined techniques of time-resolved and steady-state (UV-vis, IR) spectroscopies provide definitive identification of the 1:1 complex of the aromatic hydrocarbon with nitrosonium, *i.e.* [ArH, NO⁺], as the relevant intermediate that is derived from nitrogen dioxide (eq 7). Let us now consider the ready formation of these transient species in the context of the well-known reversible association of nitrogen dioxide primarily to the nitrogen-nitrogen bonded dimer.³⁰ Infrared analyses have established by matrix isolation and high-pressure techniques³¹ the coexistence of small (indefinite) amounts of the nitrogen-oxygen bonded isomer, presumably formed via the head-to-tail coupling of nitrogen dioxide, *i.e.*



(30) (a) Brunning, J.; Frost, M. J.; Smith, I. W. M. *Int. J. Chem. Kinet.* 1988, 20, 957. (b) Redmond, T. F.; Wayland, B. B. *J. Phys. Chem.* 1968, 72, 1626. (c) Vosper, A. J. *J. Chem. Soc. A* 1970, 2191. (d) James, D. W.; Marshall, R. C. *J. Phys. Chem.* 1968, 72, 2963. (e) Boughriet, A.; Wartel, M.; Fischer, J. C.; Bremard, C. *J. Electroanal. Chem.* 1985, 190, 103.

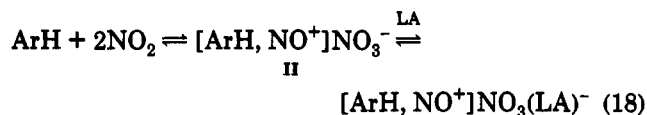
(31) Pinnick, D. A.; Angew, S. F.; Swanson, B. I. *J. Phys. Chem.* 1992, 96, 7092.

Significantly, the nitrito dimer in eq 16 has been shown to afford the disproportionated ion pair NO⁺NO₃⁻.³² Although such a heterolysis of the N-O bond is unlikely to be important in nonpolar media such as dichloromethane, the complexation of the nitrosonium moiety by an added aromatic hydrocarbon can promote ion-pair formation as II.



Thus, the formation constant in eq 6a of aromatic EDA complexes derived from NO⁺BF₄⁻ and electron-rich aromatic donors such as hexamethylbenzene can be as large as K_{EDA} = 3 × 10⁴ M⁻¹.¹⁴ Such a selective complexation of the NO⁺ moiety provides the driving force to significantly shift the disproportionation equilibrium in eq 17 from the uncharged dinitrogen tetraoxide to the ion-paired nitrosonium salt. [The stabilizing effect of ionic complexation is also evident in the dark red solutions of the hexamethylbenzene complex [HMB, NO⁺]BF₄⁻ that can be readily prepared (in excess of 0.4 M) in dichloromethane in which NO⁺BF₄⁻ alone is insoluble.] Since the previous study¹⁴ established the strong dependence of the complexation constant K_{EDA} (eq 6a) for NO⁺ on the aromatic donor strength, as evaluated by the ionization potential (Table 4, column 2), the extent of the ionic disproportionation of nitrogen dioxide in eq 17 is experimentally observed as strongly varying intensities of the charge-transfer absorption and the N-O stretching bands of II in the UV-vis and IR spectra, respectively. The results in Table 9 indicate how the increasing (steady-state) importance of the relevant [ArH, NO⁺] species is quantitatively related to the enhanced donor strengths of the various methylarenes examined in this study.


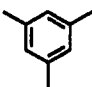
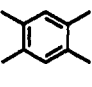
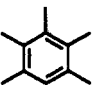
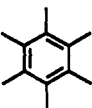
Spectral (UV-vis, IR) analyses in Table 4 and Figure 4 show that the formation of [ArH, NO⁺] is greatly promoted by the addition of antimony pentachloride to a solution of methylarene and nitrogen dioxide. This Lewis acid (LA), in common with aluminum chloride and ferric chloride, provides additional driving force for the ionic disproportionation of nitrogen dioxide via coordination to the anionic nitrate moiety,²⁶ *i.e.*



II. The Transient Nitrosonium EDA Complex II as the Critical Intermediate. The [ArH, NO⁺] complexes generated in eqs 17 and 18 are transient species, which are spontaneously transformed on standing (in the dark) to the various types of nitration products described in eqs 1-5. Indeed, there is a direct correlation between the concentration of [ArH, NO⁺], as indicated by the intensity of the charge-transfer bands in Table 4, and the temperature/time conversion in Tables 1-3 and Figure 2—both in the presence as well as absence of Lewis acid promoters. As such, we conclude that the nitrosonium EDA complex II is the critical precursor directly respon-

(32) (a) Parts, L.; Miller, J. T., Jr. *J. Chem. Phys.* 1965, 43, 136. (b) Bontempelli, G.; Mazzocchin, G.-A.; Magno, F. *Electroanal. Chem. Interfac. Electrochem.* 1974, 55, 91. (c) Wartel, A.; Boughriet, A.; Fischer, J. C. *Anal. Chim. Acta* 1979, 110, 211.

Table 9. Ionic Disproportionation of Nitrogen Dioxide by Various Aromatic Donors^a

					
methylarene					
ionization potential, eV	8.44	8.42	8.05	7.92	7.85
K_{DISP} , ^b M ⁻¹	6.0×10^{-3}	1.0×10^{-2}	7.5×10^{-2}	0.9	5.0
ΔG°_{DISP} , kcal mol ⁻¹	2.8	2.5	1.4	0.05	-0.9

^a Evaluated from K_{DISP} for the mesitylene EDA complex in Table 5 and the values of K_{EDA} for aromatic donors in ref 14. ^b For eq 7.

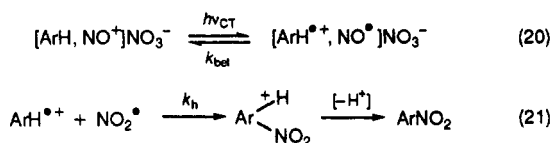
sible for the *thermal nitrations* in eqs 1–5, e.g.³³



In order to ascertain how the complicated (redox) change in eq 19 leads to aromatic nitration, let us first consider the mechanism of the corresponding charge-transfer nitration (Table 6). From a mechanistic perspective, such a photoinduced process allows the use of time-resolved spectroscopic methods to observe the reactive intermediates that are directly responsible for aromatic nitration in the following way.

III. Mechanism of Charge-Transfer Nitration with Nitrogen Dioxide. The time-resolved spectra in Figure 6 and Table 8 demonstrate that photochemical activation of the nitronium EDA complex II via the irradiation of the charge-transfer absorption band ($h\nu_{CT}$) produces the aromatic radical cation ($\text{ArH}^{\bullet+}$),²⁹ as presented in Table 8. As such, the most direct pathway to aromatic nitration proceeds via the homolytic coupling (k_h) of the aromatic radical cation with nitrogen dioxide (eq 21),³⁴ since the Wheland intermediate subsequently undergoes very rapid deprotonation,³⁵ *i.e.*

Scheme 1



According to Scheme 1,³⁶ the photoefficiency of charge-transfer nitration is limited by the rate at which the aromatic radical cation suffers homolytic coupling (k_h) relative to back-electron transfer (k_{bet}), *i.e.*, $\Phi_P \approx (k_h[\text{NO}_2^\bullet]) / (k_h[\text{NO}_2^\bullet] + k_{bet})$. For $\Phi_P = 0.1$ in Table 7, the magnitude of $[\text{NO}_2^\bullet]$ is estimated to be $< 5 \times 10^{-2} \text{ M}$ ³⁷

(33) Note the formation of nitrous acid in eq 19 is stoichiometrically equivalent to the formation of dinitrogen tetraoxide in eq 1 or nitric oxide in eq 2, as described in the Experimental Section.

(34) (a) Kim, E. K.; Bockman, T. M.; Kochi, J. K. *J. Am. Chem. Soc.* 1993, 115, 3091. (b) Independent laser flash photolysis studies of aromatic EDA complexes with nitronium $[\text{ArH}, \text{NO}^+]$ have shown that the photolytically generated radical ion pair $[\text{ArH}^{\bullet+}, \text{NO}^\bullet]$ only undergoes back-electron transfer. No product formation was observed for ArH = hexamethylbenzene, pentamethylbenzene, durene, and *p*-xylene. See: Bockman, T. M. et al. in ref 29.

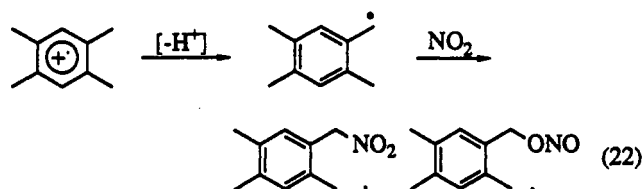
(35) (a) Melander, L.; Saunders, W. H., Jr. *Reaction Rates of Isotopic Molecules*; Wiley: New York, 1980; p 162ff. (b) As applied to charge-transfer nitration, see: Bockman, T. M.; Kochi, J. K. *J. Phys. Org. Chem.*, in press.

(36) (a) Note that the mixture of HNO_3 and NO produced in Scheme 1 is equivalent to N_2O_3 and H_2O in eq 1. See: Bosch, E.; Rathore, R.; Kochi, J. K. *J. Org. Chem.*, in press. See also: Wartel, A. et al. in ref 32c. Forsythe, W. R.; Giaque, W. F. *J. Am. Chem. Soc.* 1942, 64, 48. (b) The rate of diffusive separation of the radical pair resulting from eq 20²⁹ is neglected in Scheme 1.

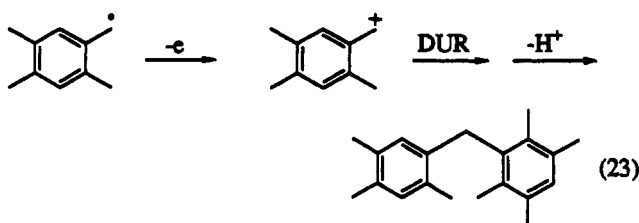
(37) This value for the upper limit of $[\text{NO}_2]$ derives from the simplifying assumption that the diffusive rate constant is slower than that for back-electron transfer (otherwise the kinetics cannot be solved in closed form).

based on typical values of $k_{bet} \approx 5 \times 10^8 \text{ s}^{-1}$ ²⁹ and $k_h \approx 10^9 \text{ s}^{-1}$.^{34a} Such low (quasi-steady-state) concentrations of monomeric species are reasonable, in view of the extensive dimerization of nitrogen dioxide in nonpolar media.³⁰

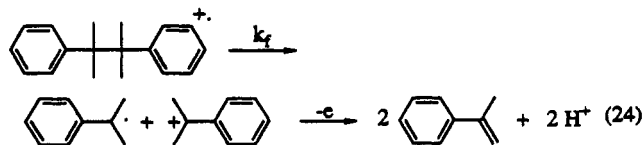
The aromatic radical cation $[\text{ArH}^{\bullet+}]$ also accounts for the myriad of "nonconventional" byproducts³⁸ that accompany charge-transfer nitration of various aromatic hydrocarbons. For example, the radical cations derived from the methylbenzenes are highly susceptible to α -deprotonation,³⁹ which leads to the side chain substitution of durene (DUR) in eq 11, *i.e.*



and the same intermediates are responsible for the oxidative dimerization⁴⁰ to the diarylmethanes in Table 6, e.g.⁴¹



Moreover, the rapid mesolytic cleavage of the radical-cation of bicumene⁴³ is responsible for the high yields of α -methylstyrene (eq 12) obtained from the treatment of this aromatic hydrocarbon with nitrogen dioxide, *i.e.*



(38) See: (a) Hartshorn, S. R. *Chem. Soc. Rev.* 1974, 3, 167. (b) Suzuki, H. *Synthesis* 1977, 217.

(39) Masnovi, J. M.; Sankararaman, S.; Kochi, J. K. *J. Am. Chem. Soc.* 1989, 111, 2263.

(40) (a) Yoshida, K. *Electrooxidation in Organic Chemistry*; Wiley: New York, 1984; p 133. (b) Lau, W.; Kochi, J. K. *J. Am. Chem. Soc.* 1984, 106, 7100.

(41) Electron loss from benzylic radicals is rapid,⁴² and the oxidant in these systems may be NO^+ or NO_2 .

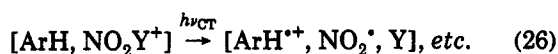
(42) Rollick, K.; Kochi, J. K. *J. Am. Chem. Soc.* 1982, 104, 1319; *J. Org. Chem.* 1982, 47, 435.

(43) (a) Reichel, L. W.; Griffin, G. W.; Muller, A. J.; Das, P. K.; Ege, S. N. *Can. J. Chem.* 1984, 62, 424. (b) Albini, A.; Spreti, S. *J. Chem. Soc., Perkin Trans. 2* 1987, 1175.

Most importantly, the fast (estimated) rate constant⁴⁴ of $k_f > 10^8 \text{ s}^{-1}$ accounts for the singular lack of competition from aromatic nitration via the homolytic coupling (k_h) in Scheme 1.

In essence, charge-transfer nitration with nitrogen dioxide, as delineated in Scheme 1, utilizes actinic energy to generate the aromatic radical cation as the reactive intermediate for homolytic coupling with NO_2 in eq 21. As such, it is conceptually related to the photoinduced electron transfer of aromatic hydrocarbons with nitronium carriers such as tetranitromethane^{39,45} and *N*-nitropyridinium salts,⁴⁶ in which the reactive radical ion pair is produced directly in the course of charge-transfer activation, *i.e.*²⁸

Scheme 2



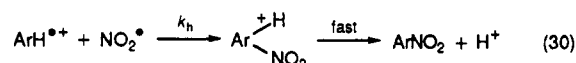
where Y = pyridine, trinitromethide, *etc.* Thus, the subsequent formation of the Wheland intermediate via the homolytic coupling of the aromatic radical cation with NO_2^{\bullet} is stoichiometrically equivalent to that in Scheme 1 (eq 21).⁴⁷ Indeed, the direct and detailed comparison shows that the product compositions, including the isomeric distribution of the nitroarenes as well as the other "nonconventional" byproducts obtained in Table 6, bear an unmistakable resemblance to those previously obtained from charge-transfer nitrations of the same aromatic hydrocarbons with *N*-nitropyridinium³⁴ and tetranitromethane.³⁹ Despite the fact that the electron-transfer mechanisms in Schemes 1 and 2 differ in the composition of the radical pair; *i.e.*, $[\text{ArH}^{\bullet+}, \text{NO}^{\bullet}]$ and $[\text{ArH}^{\bullet+}, \text{NO}_2^{\bullet}]$ similar product compositions are obtained. We therefore conclude that the kinetics distinction imposed by the subsequent diffusive separations and encounters of radical pairs is not highly relevant to the ultimate product composition.⁴⁷

IV. The Thermal Nitration of Aromatic Hydrocarbons with Nitrogen Dioxide. The photochemical and thermal nitrations of aromatic hydrocarbons with nitrogen dioxide are carried out under essentially the same experimental conditions—the charge-transfer activation being merely effected with light at lower temperatures where competition from the thermal process is unimportant. For this reason, it is particularly noteworthy that the thermal nitration at 25 °C (in the dark) and charge-transfer nitration at -78 °C (with $\lambda_{\text{exc}} > 415 \text{ nm}$) lead to the same products in Tables 1 and 6, respectively. In both cases, a common mix of side chain (NO_2 and ONO_2) substitutions result from hexamethylbenzene, pentamethylbenzene, and durene, and ring nitration is the

exclusive result from mesitylene, pseudocumene, and *m*-xylene. Such a coincidence is not fortuitous, since the thermal and charge-transfer nitration of *o*- and *p*-xylene both lead to a uniquely complex mixture of products resulting from simultaneous ring nitration, side chain (NO_2 and ONO_2) substitution, and oxidative dimerization (see Experimental Section for details.)

In view of the striking similarities that we consistently delineated in (a) the isomeric product distributions, (b) nuclear versus side chain nitration, and (c) NO_2/ONO_2 substitutions, the most direct formulation of thermal nitration invokes the production of the same $[\text{ArH}^{\bullet+}]$ intermediate in the dark, *i.e.*

Scheme 3



Since the electron transfer ($\log k_E$) in the nitronium EDA complex represents the adiabatic counterpart to the photochemical activation ($h\nu_{\text{CT}}$), the radical ion pair in eq 28 is akin to that in eq 20. Following the diffusive separation (k_{diff}) in eq 29, the aromatic radical cation is free to engage in the same diverse reactions (*i.e.*, eqs 21–24) leading to the characteristic product array from ring nitration and other nonconventional processes.³⁸

Since the steady-state concentration of the $[\text{ArH}^{\bullet+}]$ intermediate in Scheme 3 is perforce low, the direct methods for its observation are limited. However, the isolation of the dimeric binaphthyl (14%) in the course of methylnaphthalene nitration with nitrogen dioxide (eq 5) is circumstantial evidence for the facile production of the radical cation.⁴⁹ Indeed, the driving force for electron transfer in eq 27 is mildly endergonic for methylnaphthalene and for the methylarenes: hexamethylbenzene, durene, mesitylene, and even xylene.²⁹ Thus, the rapid followup reactions in eqs 21–24 are sufficient to drive the electron-transfer of these aromatic donors to completion.⁵⁰ On the other hand toluene is a significantly weaker electron donor⁵¹ and reacts with nitrogen dioxide only in the presence of Lewis acids. In the latter case, the low conversions to the isomeric nitrotoluenes in Table 3 may also derive via the incursion of an alternative disproportionation of nitrogen dioxide to nitronium nitrite.⁵²

In a broader context, the electron-transfer mechanism proposed in Scheme 3 for the thermal nitration of aromatic hydrocarbon with nitrogen dioxide is a minor variant of the more common nitrations with nitric acid that are catalyzed by nitrous acid (*i.e.*, NO^+).^{1,2} The electron-

(44) Maalak, P.; Chapman, W. H., Jr. *J. Org. Chem.* 1990, 55, 6334.

(45) (a) Altukhov, K. V.; Perekalin, V. V. *Russ. Chem. Rev.* 1976, 45, 1052. (b) Sankararaman, S.; Haney, W. A.; Kochi, J. K. *J. Am. Chem. Soc.* 1987, 109, 5235, 7824.

(46) (a) Olah, G. A.; Narang, S. C.; Olah, J. A.; Pearson, R. L.; Cupas, C. A. *J. Am. Chem. Soc.* 1980, 102, 3507. (b) Kim, E. K.; Lee, K. Y.; Kochi, J. K. *J. Am. Chem. Soc.* 1992, 114, 1756.

(47) Kinetic equivalency must consider the diffusive rates of radical and radical-ion pairs.

(48) It is possible (but deemed unlikely) that some nitroarene is formed via the corresponding nitroso derivative which is oxidatively converted under conditions of the thermal nitration (but not CT nitration), as described in the Experimental Section.

(49) See: Radner, F. in ref 20.

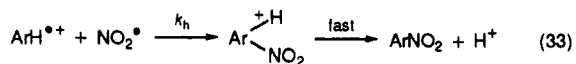
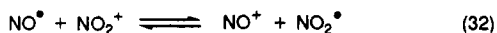
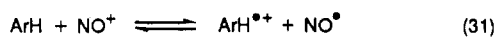
(50) For the kinetics, see: Bard, A. J.; Faulkner, L. R. *Electrochemical Methods*; Wiley: New York, 1980; p 429ff.

(51) For example, the ionization potential of toluene (8.82 eV) is 0.38 eV higher than *p*-xylene and almost 1 eV higher than hexamethylbenzene. See: Howell, J. O. et al. in ref 21.

(52) (a) Compare Evans, J. C. et al. in ref 8d. (b) A reviewer has suggested that the α -nitrotoluene produced in the thermal reaction of toluene with NO_2 may (also) be formed by hydrogen atom abstraction by NO_2 followed by radical coupling. See: Titov, A. I. in ref 4. Pryor, W. A. et al. in ref 5.

transfer mechanism for the latter, based on kinetics and CIDNP studies,⁵³ is summarized below.⁵⁴

Scheme 4



[Note the rapid preequilibrium step with nitric acid, *i.e.*, $\text{HNO}_3 + \text{H}^+ \rightleftharpoons \text{NO}_2^+ + \text{H}_2\text{O}$, is responsible for the presence of the nitronium ion in eq 32.^{55,56}]

According to Schemes 3 and 4, the stoichiometric and catalytic processes for aromatic nitration by nitrogen dioxide and by nitric acid (with NO^+) share the homolytic coupling of $\text{ArH}^{\bullet+}$ as the common route to the Wheland intermediate in eqs 30 and 33, respectively. It is thus the facile reoxidation of NO^{\bullet} by nitric acid to regenerate nitronium in the catalytic process (Scheme 4, eq 32⁵⁶) that provides a direct connection to the stoichiometric nitration, in which the relevant oxidant is derived via the disproportionation of nitrogen dioxide (Scheme 3, eq 27).

Summary and Conclusions

Nitrogen dioxide undergoes a rapid, reversible disproportionation with aromatic hydrocarbons to form the metastable EDA complex II of the composition $[\text{ArH}, \text{NO}^+]\text{NO}_3^-$ according to eq 7. On standing, the red solution of $[\text{ArH}, \text{NO}^+]\text{NO}_3^-$ is bleached, and it yields the various nitration products from the methylbenzenes listed Table 1. The least reactive toluene is converted to the isomeric nitrotoluenes only upon the addition of Lewis acid promoters (LA). Quantitative isolation of the red solid III of composition $[\text{ArH}, \text{NO}^+]\text{NO}_3(\text{LA})^-$ points to the 1:1 interaction of the aromatic hydrocarbon with nitronium, *i.e.*, $[\text{ArH}, \text{NO}^+]$, as the critical (charge-transfer) component for aromatic nitration.

The deliberate irradiation of the red solution at low temperature (-78°C) with filtered light selected to activate only $[\text{ArH}, \text{NO}^+]\text{NO}_3^-$ represents an alternative procedure for aromatic nitration (Table 6). Time-resolved spectroscopy establishes such a photoinduced nitration to proceed via the aromatic cation radicals in Table 8, since it derives directly from the vertical (charge-transfer) excitation of the precursor complex II to the radical pair $[\text{ArH}^{\bullet+}, \text{NO}^{\bullet}]$. According to Scheme 1, the subsequent homolytic coupling of $\text{ArH}^{\bullet+}$ with nitrogen dioxide leads to the usual Wheland intermediate for aromatic nitration (eq 21).

Thermal activation of the precursor EDA complex II via the adiabatic electron transfer in $[\text{ArH}, \text{NO}^+]$ leads to the same radical pair $[\text{ArH}^{\bullet+}, \text{NO}^{\bullet}]$ in Scheme 3. The homolytic reactions of $\text{ArH}^{\bullet+}$ are sufficiently rapid to drive

the moderately endergonic electron transfer for many methylbenzenes to completion. Most importantly, the paramagnetic intermediates are the same as those produced in the electron-transfer pathway in Scheme 4 for aromatic nitrations carried out with nitric acid (that contains nitrous acid).⁵⁴

These studies underscore the facility with which the nitrogen oxides are (inter)converted by one-electron transfer among nitric acid, nitrogen dioxide, nitronium, and nitric oxide in nitrogen (V), -(IV), -(III), and -(II) oxidation states, respectively. From a preparative viewpoint, extreme caution is required to ensure the purity of the proper nitrating agent to circumvent any complication from the efficient electron-transfer catalysis.^{57,58}

Experimental Section

Materials. The purification of nitrogen dioxide,¹³ nitric oxide,²⁹ nitronium tetrafluoroborate²⁹ and nitronium hexachloroantimonate¹⁴ has been described. The aromatic hydrocarbons used in this study and the products listed in Table 1, 2, 3, and 4 were available from previous studies.^{14,39,59} Dichloromethane, acetonitrile, nitromethane, and nitroethane were purified as described previously.²⁹ Antimony pentachloride, aluminum trichloride, and phosphorus pentachloride (Aldrich) were used as received.

Charge-Transfer Nitration of the Methylbenzenes with Nitrogen Dioxide. General Procedure. Typically, two identical dichloromethane solutions of the aromatic hydrocarbon and NO_2 were prepared in identical 25-mL Schlenk tubes. Thus, a solution of durene (135 mg, 1.00 mmol) in dichloromethane (7 mL) was prepared in each of the Schlenk tubes which were then cooled under a flow of argon to -78°C in a dry ice/acetone bath. Nitrogen dioxide (0.22 mL, 7.0 mmol) was added directly into each solution with an all-glass syringe (fitted with a platinum needle), and it resulted in an immediate deep red color. Both tubes were then sealed, and one was wrapped in aluminum foil to serve as the unirradiated dark control. Both tubes were placed in an acetone-filled Dewar maintained at $-70^\circ\text{C} \pm 3^\circ\text{C}$ with an immersion cooler. The unwrapped solution was irradiated with focused light from a medium-pressure mercury lamp passed through an aqueous IR filter and a 415-nm cutoff filter. This procedure ensured that only the CT band was irradiated. The UV-vis absorption spectrum was periodically monitored. It showed a steady bleaching of the color. After 17 h irradiation, the red color had faded and the solution was greenish. (The UV-vis absorption spectrum which was recorded at -78°C revealed a broad absorption centered at $\lambda_{\text{max}} = 690 \text{ nm}$ for N_2O_3 that was formed by complexation of the NO generated in the reaction with the unreacted NO_2 .) The irradiated and control solutions were then simultaneously worked up. Each solution was separately poured into a vigorously stirred mixture of ether (40 mL) and saturated aqueous sodium bicarbonate. [The ether contained pentamethylbenzene (20 mg) which served as internal standard for both GC and HPLC analysis. This procedure was also used to confirm that reaction did not occur during workup.] The ether was separated, and the aqueous layer neutralized with dilute HCl and extracted with ether (20 mL). The ether portions were combined, dried, and filtered, and the solvent was removed in vacuo. The colorless residue was analyzed by quantitative GC, HPLC, and GC-MS.

(53) Giffney, J. C.; Ridd, J. H. *J. Chem. Soc., Perkin Trans. 2* 1979, 618.

(54) For a summary, see: Ridd, J. H. *Chem. Soc. Rev.* 1991, 20, 149.

(55) Ingold, C. K. *Structure and Mechanism in Organic Chemistry*, 2nd ed.; Cornell University Press: Ithaca, NY, 1953.

(56) Since the nitronium ion reacts at diffusion-controlled rates with even mediocre donors such as benzene,² it is unlikely to exist in steady-state concentrations sufficient for that required in eq 32 (even at high concentrations). Accordingly, we suggest an alternative chain-transfer step, involving the direct oxidation of nitric oxide with nitric acid to produce dinitrogen trioxide (and water)³⁶ which undergoes ready homolysis to nitrogen dioxide and nitric oxide.¹⁸ (The overall transformation thus corresponds to the dehydration of nitric acid.)

(57) Note that aromatic nitrations with nitric acid in organic solvents that yield products much like those in Tables 1–3 may involve NO^+ catalysis. See: (a) Mishina, T. *J. Sci. Hiroshima Univ. Ser. A* 1980, 44, 157. (b) Suzuki, H.; Mishina, T.; Hanafusa, T. *Bull. Chem. Soc. Jpn.* 1979, 52, 191. (c) Suzuki, H.; Nakamura, K. *Bull. Chem. Soc. Jpn.* 1970, 43, 473. (d) Nakamura, K. *Bull. Chem. Soc. Jpn.* 1971, 44, 133. (e) Dincturk, S.; Ridd, J. H. *J. Chem. Soc., Perkin Trans. 2* 1982, 965. Hanna, S. B. et al. in ref 19.

(58) The caveat by Ridd⁵⁴ is "... unless high concentrations of nitrous acid traps are used, most preparative nitrations of such compounds probably proceed mainly through the nitrous acid pathway..." *i.e.*, Schemes 3 and 4.

(59) Kim, E. K.; Kochi, J. K. *J. Org. Chem.* 1993, 58, 786.

Acknowledgment. We thank S. M. Hubig for assistance with the time-resolved spectroscopic studies and the National Science Foundation, Robert A. Welch Foundation, and the Texas Advanced Research Program for financial assistance.

Supplementary Material Available: The materials and instrumentation used, the thermal nitration of hexamethylbenzene, pentamethylbenzene, durene, mesitylene, 1,2,4-trimethylbenzene, *p*-xylene, *m*-xylene, *o*-xylene, toluene, benzene, and 1-methylnaphthalene are described in detail. The determination of the stoichiometry of the nitration of aromatic hydrocarbons and the effect of nitric oxide, tetra-*n*-butylammonium nitrate, and 4-methyl-2,6-di-*tert*-butylpyridine on the reaction is described as is the product stability under the reaction conditions. The measurement of the charge-transfer absorption spectra of the methylbenzenes with nitrogen dioxide and nitrosonium

tetrafluoroborate and the effect of nitric oxide on the spectra are described as are the vibrational spectra of these complexes. The charge-transfer nitration of the methylbenzenes durene, pentamethylbenzene, hexamethylbenzene, mesitylene, 1,2,4-trimethylbenzene, *m*-xylene, *o*-xylene, *p*-xylene, toluene, and benzene with nitrogen dioxide, the product stability under the reaction conditions, the quantum yields for charge-transfer nitration with nitrogen dioxide, and the charge-transfer reaction of bicumenes with nitrogen dioxide are described in detail. The complex formation on addition of antimony pentachloride to the methylbenzenes and nitrogen dioxide, the effect of the Lewis acids antimony pentachloride, aluminum trichloride, ferric chloride, and phosphorus pentachloride on the nitration of benzene and toluene with nitrogen dioxide are described (23 pages). This material is contained in libraries on microfiche, immediately follows this article in the microfilm version of the journal, and can be ordered from the ACS; see any current masthead page for ordering information.